

# Large language model-enhanced Bayesian optimization for parameter identification of lithium-ion batteries

Xiao Kuai<sup>a</sup>, Jia-Hui Ren<sup>a</sup>, Bing-Chuan Wang<sup>a</sup>, Yun Feng<sup>b</sup>

<sup>a</sup>*Central South University, Changsha 410083, China*

<sup>b</sup>*Hunan University, Changsha 410082, China*

## Abstract

Lithium-ion batteries play a vital role in modern energy storage systems, with their performance and safety critically dependent on the accurate identification of key parameters. Bayesian optimization (BO), renowned for its effectiveness in data-scarce and complex nonlinear scenarios, has emerged as a powerful tool for parameter identification. However, the effectiveness of BO largely depends on the quality of surrogate models and sampling efficiency, posing significant challenges in low-sample contexts. Recently, large language models (LLMs) have shown great promise when integrated with BO, owing to their exceptional few-shot learning capabilities and their ability to extract meaningful insights from sparse data. This paper is the first attempt to apply the combination of LLMs and BO for the efficient parameter identification of lithium-ion batteries. By representing BO components in natural language, the presented LLM-enhanced BO (LLMBO) establishes a well-informed warm start that directly generates promising initial parameter estimates for the pseudo-two-dimensional battery model, thereby accelerating the parameter identification process. Moreover, by leveraging the few-shot learning and contextual inference capabilities of LLMs, LLMBO effectively incorporates prior domain knowledge to guide early-stage exploration, resulting in more accurate and efficient identification of lithium-ion battery parameters. Experimental results show that LLMBO outperforms the traditional BO and other heuristic algorithms in terms of both accuracy and efficiency, demonstrating its significant advantages. Additionally, we compare the performance of different kinds of LLMs in parameter identification tasks, providing valuable insights into their effectiveness.

**Keywords:** Large language models, Bayesian optimization, Parameter identification, Lithium-ion battery.

## 1. Introduction

### 1.1. Background

Lithium-ion batteries play a crucial role in modern energy storage systems [1, 2], with their performance and safety heavily influenced by various factors, especially the accurate identification of key parameters [3]. The accurate assessment of these parameters depends not only on the physical characteristics of the battery, such as diffusion coefficients, open-circuit voltage curves, and thermal properties, but also on the chemical reactions occurring within the battery and the current-voltage relationship [4, 5]. These parameters are crucial for enhancing battery efficiency and safety, particularly during charge-discharge cycles and fast charging. However, some key parameters cannot be directly measured, as measuring them would cause damage. Therefore, parameter identification assisted by battery models is more cost-effective.

Among the various models, electrochemical models are distinguished by their high accuracy, as they effectively capture a battery's internal physical phenomena. The pseudo-two-dimensional (P2D) model is widely recognized as one of the most representative electrochemical models, serving as the foundation for many other models. Building on this foundation, recent years have seen significant advancements in both model development and parameter identification methodologies. Numerous studies have combined the P2D model with data-driven

approaches to tackle these challenges. These efforts aim to improve both the precision of key parameter identification and the effectiveness of optimization processes in electrochemical systems. In summary, effective parameter identification has become crucial for enhancing lithium-ion battery performance and extending its lifespan [6].

### 1.2. Parameter identification methods

Currently, parameter identification methods for lithium-ion batteries can be primarily categorized into three classes. While these approaches have achieved notable success in specific scenarios, each exhibits certain limitations that restrict their ability to balance efficiency and accuracy.

#### 1.2.1. Experimental methods

These methods directly measure the electrical and thermal properties of the battery. Common experimental techniques include pulse testing and constant current charging. Lain et al. [7] applied short current pulses to extract the dynamic response of the battery, thus identifying parameters such as internal resistance and capacity. Rod-riuez-Cea et al. [8] used a constant current to charge or discharge the battery and estimated parameters based on voltage changes. Experimental methods are time-consuming and require specialized equipment. Furthermore, the experimental process can cause irreversible effects on the battery, such as capacity degradation.

### 1.2.2. Model-based methods

The P2D model, grounded in porous electrode theory [9], concentrated solution theory [10], and Maxwell-Stefan multi-component diffusion theory [11], enables physics-based optimization of cell design parameters and provides critical insights into internal electrochemical phenomena. Despite its high accuracy, practical challenges persist due to the model’s extreme computational complexity and heavy reliance on experimental data. To address these limitations, researchers have pursued two primary improvement strategies. The first involves reduced-order models (ROMs), such as the single-particle model (SPM) [12, 13], which simplifies electrode dynamics by representing each electrode as a single active particle and neglecting electrolyte-phase transport, thereby drastically reducing computational costs [14]. However, SPM’s omission of electrolyte concentration polarization leads to significant voltage prediction errors under high-current-rate conditions. Another ROM, the multi-scale multi-domain model [15], partitions the spatial domain into particle, electrode, and cell-scale subdomains, exchanging averaged field quantities to reduce coupled equation counts. While computationally efficient, this approach sacrifices spatial resolution, failing to resolve localized gradients such as abrupt electrolyte potential transitions.

The second strategy focuses on advanced numerical methods. In [16], the finite volume method combined with backward Euler discretization utilizes the tridiagonal matrix algorithm to accelerate spatiotemporal domain solutions and reduce iterative complexity. In [17, 18, 19], the orthogonal collocation method approximates the solutions of partial differential equations using orthogonal polynomials, transforming them into differential-algebraic equations. Despite improved computational speed, these methods remain susceptible to parameter sensitivity and high-dimensional nonlinear coupling [20].

In summary, although these strategies partially alleviate computational burdens, ROMs still fall short in accurately predicting key internal states [14]. Moreover, numerical methods continue to struggle with balancing parameter robustness and computational efficiency, highlighting the need for hybrid approaches to bridge the gap between model fidelity and practical applicability.

### 1.2.3. Data-driven methods

With the development of machine learning and deep learning technologies, data-driven methods have become crucial tools in parameter identification. Machine learning techniques such as support vector machines [21], genetic algorithms (GAs) [22], and particle swarm optimization (PSO) [23] can learn battery behavior patterns from large sets of experimental data, even without an explicit physical model. Deep learning techniques, such as convolutional neural networks [24], are capable of automatically extracting complex features from battery data, making them particularly suitable for handling nonlinear and high-dimensional problems. However, data-driven methods require high-quality and large quantities of data, and in scenarios with limited samples, they may suffer from overfitting or poor generalization performance. Additionally, the training process demands substantial computational resources and time.

Bayesian optimization (BO), as a data-driven optimization method, offers significant advantages in handling data-scarce and nonlinear problems. Compared to traditional machine learning methods, BO seamlessly integrates surrogate models and optimization algorithms, conducting efficient global searches that avoid local optima and result in more accurate parameter identification. The surrogate model in BO maximizes information utilization when evaluating expensive objective functions, making it especially suited for tasks with limited samples or high computational costs.

### 1.3. Research gap and motivation

Although BO shows promise for parameter identification, its efficiency as a high-performance optimization framework largely depends on the quality of the surrogate model and the effectiveness of candidate sampling in rapidly identifying high-potential regions. Since BO is designed for scenarios with limited samples, constructing an accurate surrogate model from sparse data remains a significant challenge. Furthermore, this model can be highly sensitive to mis-specifications; even minor inaccuracies in model representation may introduce significant biases, thereby distorting the sampling of potential solutions. When incorporating prior knowledge, an additional challenge emerges—effectively transferring insights about correlations within the optimization space to new tasks.

At the core of these challenges is the accurate learning of the objective function and effectively generating candidate solutions from very few samples [25]. This scenario is commonly referred to as the few-shot scenario, where the environment demands rapid learning and generalization from very few samples. Interestingly, this challenge in few-shot learning aligns well with the strengths of large language models (LLMs). Pre-trained on internet-scale data, modern LLMs exhibit remarkable generalization capabilities from limited samples, enabling them to excel in few-shot prediction and generation [26, 27, 28, 29, 30], as well as contextual understanding [31, 32]. Their exceptional sample efficiency is partly due to the use of encoded priors [33, 34]. Recently, Liu et al. [35] combined LLMs with BO, a strategy particularly well-suited for parameter identification, which serves as a key inspiration for our work.

### 1.4. Contributions

Motivated by these considerations, we adapt and modify an LLM-enhanced Bayesian optimization (LLMBO) framework [35] to enable fast parameter identification of lithium-ion batteries. In LLMBO, the components of BO are represented in natural language, enabling efficient preheating, and leveraging the extensive prior knowledge and few-shot learning capabilities of LLMs to assist in identifying the optimal battery parameters. The main contributions are summarized as follows.

1. We pioneer the application of the LLMBO framework to lithium-ion battery parameter identification, proposing an innovative solution for strongly coupled parameters in the P2D model. By encoding electrochemical parameter

semantics through natural language, we develop hierarchical surrogate models and design a physics-constrained sampling strategy.

2. In LLMBO, LLMs are employed to warm-start BO by transferring prior knowledge relevant to parameter identification. Consequently, this approach operates without the need for task-specific pre-training or the extraction of structured outputs from the P2D model, thereby enhancing identification efficiency.
3. This study presents the first systematic analysis of performance differences among multiple LLMs in parameter identification of lithium-ion batteries. Experimental results reveal that GPT-4o and DeepSeek-R1, owing to their advanced contextual reasoning capabilities, outperform other models. These findings provide valuable insights for selecting appropriate LLMs in parameter identification tasks.
4. Experimental results show that LLMBO outperforms the traditional BO and other heuristic algorithms in terms of both accuracy and efficiency, demonstrating its significant advantages.

### 1.5. Organization

The rest of this paper is organized as follows. Section 2 introduces some preliminaries, including the P2D model, BO, and the parameter identification problem. The proposed method is illustrated in Section 3. Section 4 details the experimental study, and concluding remarks are provided in Section 5.

## 2. Preliminaries

### 2.1. P2D model

The P2D model is widely regarded as one of the most representative electrochemical models [36, 37]. This model assumes that each point on the electrode contains a spherical particle representing the active material, resulting in a spatial dimension for the electrode thickness and another spatial dimension for the radius of each particle. This model has been extensively studied and serves as a powerful tool for evaluating, optimizing, and predicting battery performance. The details of the P2D model can be found in [36, 37].

The parameters of the P2D model characterize the physical, chemical, and electrochemical properties of the battery. The reliability of the P2D model heavily depends on the accuracy of these parameters, which are inherently specific to each battery design—whether in terms of geometry or material composition. Consequently, parameter values are not universally transferable across different battery configurations. This makes the identification of an appropriate parameter set for a given battery one of the fundamental challenges in battery modeling.

The detailed parameters of the P2D model can be found in [15, 38], which are classified into static and dynamic parameters. Static parameters are determined by the materials and

geometry of the battery, and are typically provided by the manufacturer or measured directly. In contrast, dynamic parameters are closely related to the internal characteristics of the lithium-ion battery. Therefore, the identification of dynamic parameters is of greater importance under real-world conditions.

### 2.2. BO

BO is a sequential surrogate model-based approach that employs a surrogate model to approximate the objective function. Afterward, the surrogate model is updated by an infill criterion which is able to make use of full information provided by historical data. The details of BO can be found in [39, 40].

BO consists of two primary components: a surrogate model and an infill criterion. The typical optimization process begins by selecting an initial set of sample points:  $\theta_0, \theta_1, \dots, \theta_k$ , from the defined parameter space. These points are then evaluated to compute their corresponding objective function values:  $f(\theta_0), f(\theta_1), \dots, f(\theta_k)$ . A Gaussian process (GP) is employed as the surrogate model, trained on the evaluated sample set  $\mathcal{D} = \{\theta_i, f(\theta_i)\}$ , to provide both the predicted mean  $\mu_k$  and the associated uncertainty estimate  $\sigma_k$ . Based on the surrogate model, the acquisition function  $\alpha(\theta)$  is computed, and the next sampling point is selected by maximizing this function:

$$\theta_{k+1} = \arg \max_{\theta} \alpha(\theta). \quad (1)$$

where the true objective function value at  $\theta_{k+1}$  is then evaluated, and the dataset  $\mathcal{D}$  is updated accordingly.

Traditional BO, constrained by the static nature of its surrogate model, often exhibits slow convergence and struggles to adapt to dynamic search requirements. To address these limitations, we introduce LLMBO in Section 3, which integrates LLMs to enhance BO surrogate model updates and candidate sampling, thereby improving convergence speed and optimization accuracy in parameter identification tasks.

### 2.3. Parameter identification problem

This study formulates the lithium-ion battery parameter identification problem as an optimization task, with the core objective of minimizing the discrepancy between the simulated voltage outputs of the P2D model and experimentally observed values. The problem is formulated as follows:

$$\min_{\theta} f(\theta) = \frac{1}{n} \sum_{i=1}^n (U_i^{\text{ref}} - U_i)^2 \quad (2)$$

$$\underline{\theta}_j \leq \theta_j \leq \bar{\theta}_j, j = 1, 2, \dots, q \quad (3)$$

where  $\theta = [\theta_1, \theta_2, \dots, \theta_q]^T$  represents the parameter vector containing the battery model parameters to be identified,  $U^{\text{ref}}$  includes the experimentally observed voltages,  $U$  represents the reference voltages generated by the P2D model,  $U_i^{\text{ref}}$  and  $U_i$  are the  $i$ th samples of the reference voltages and the measured voltages, respectively,  $n$  is the number of samples, and  $\underline{\theta}_j$  and  $\bar{\theta}_j$  are the lower and upper bounds of the parameter  $\theta_j$ , respectively. In the parameter identification problem of lithium-ion batteries,

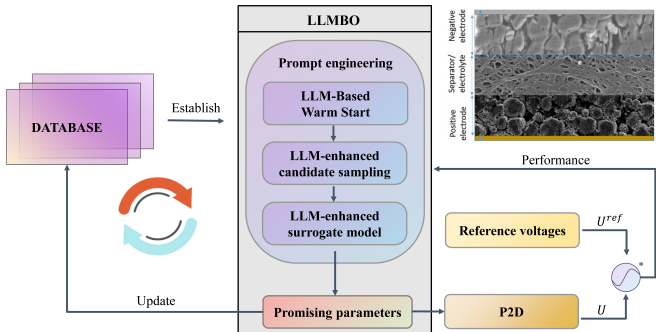


Figure 1: Framework of LLMBO for parameter identification of lithium-ion batteries.

model parameters are typically constrained by physical, chemical, and experimental conditions. Therefore, upper and lower bounds must be applied during the identification process to ensure the physical validity of the results, prevent meaningless solutions, and accelerate convergence.

The critical challenges in lithium-ion battery parameter identification stem from the inherent strong nonlinearity and multiphysics coupling effects in electrochemical models, which lead to a nonconvex objective function. Moreover, the scarcity of experimental data across diverse operating conditions, combined with the high computational cost of P2D model evaluations, further limits the efficiency of conventional parameter identification methods. The sensitivity of dynamic parameters exacerbates these challenges. Traditional approaches struggle to achieve efficient exploration under limited data and high computational costs due to their reliance on random sampling or rigid surrogate models. To address these limitations, the presented LLMBO framework integrates natural language processing-enhanced BO, combining prior knowledge-guided initialization and context-aware dynamic sampling strategies. This approach effectively addresses the dual challenges of data scarcity and computational cost, providing an innovative solution for parameter identification in complex physical systems.

### 3. Propoeds method

#### 3.1. General framework

The framework of LLMBO for parameter identification is illustrated in Figure 1, where LLMBO leverages prompt engineering to optimize the parameter set in the database and identify the optimal parameter vector. Specifically, the database is initially constructed using a random function. After a warm start, LLMBO refines the parameters in the database by identifying promising sample candidates. Following simulations with the P2D model, the objective function is evaluated, and the optimization loop updates the database with the promising parameters based on the candidate sampling. This process continues until the stopping criterion is met, at which point the optimal parameter vector from the database is returned.

This framework enables LLMs to conceptualize the components of BO through natural language processing, allowing

As an expert in [electrochemistry](#), generate an initial candidate parameter set for the [pseudo-two-dimensional model of lithium-ion batteries](#). The [lithium-ion battery parameter characteristics](#) are provided below, ensuring parameters conform to realistic [electrochemical behavior](#) regarding active material volume fraction and electrolyte properties. Parameters must satisfy material property constraints. Incorporate prior knowledge from literature and avoid invalid combinations. Prioritize generating diverse initial samples that balance exploration of valid ranges with physical feasibility.

Figure 2: Prompt for warm start.

Design a Bayesian optimization surrogate model that explicitly captures [electrochemical interactions in the P2D model](#). Construct a composite kernel function combining a radial basis function with a coupling term based on porous electrode theory. For instance, model the synergistic effects between solid-phase diffusion and electrolyte volume fraction using gradient correlation analysis. Dynamically adjust hyperparameters: shorten the kernel length scale for parameters [causing voltage transients](#), and adapt the coupling strength based on convergence trends. Validate predictions against [multi-rate experimental voltage curves](#) to ensure physical consistency.

Figure 3: Prompt for surrogate modeling.

the model to iteratively propose and evaluate promising solutions informed by historical evaluations. More specifically, this method explores how to combine contextual understanding, few-shot learning capabilities, and the domain knowledge of LLMs to improve BO. As a result, LLMBO uses in-context learning to enable effective zero-shot warm starts and improves both surrogate modeling and candidate sampling. The main components of LLMBO, including LLM-based warm start, LLM-enhanced surrogate modeling, and LLM-enhanced candidate sampling, are illustrated next.

#### 3.2. LLM-based warm start

As shown in Figure 2, LLMBO generates physically plausible initial parameter sets by encoding lithium-ion battery parameter characteristics into natural language prompts. For example, the prompt for one critical parameter may state: “The typical range of the positive electrode active material volume fraction (denotes as  $\varepsilon_{act,p}$ ) is 0.2 to 0.8, subject to the constraint  $\varepsilon_{act,p} + \varepsilon_{e,p} \leq 1$  to avoid porosity conflicts, where  $\varepsilon_{e,p}$  denotes the volume fraction of the electrolyte phase in the positive electrode.” In summary, LLMBO generates initial parameters based on these constraints:

$$\theta_0 \sim \mathcal{P}_{LLM}(\theta | \mathcal{S}) \quad (4)$$

where  $\mathcal{S}$  represents domain-specific semantic constraints and  $\mathcal{P}_{LLM}$  denotes the LLM-based parser responsible for analyzing this constraint set. This way, prior knowledge is leveraged by the LLM to interpret parameter correlations and generate initial samples. These generated parameters are subsequently filtered through boundary conditions to ensure that the initial samples fall within valid intervals.

#### 3.3. LLM-enhanced surrogate modeling

The GP kernel adopted in traditional BO often fails to capture the complex nonlinear couplings within the parameter space. To address this limitation, LLMBO introduces a composite kernel:

$$k(\theta, \theta') = \underbrace{\exp\left(-\frac{\|\theta - \theta'\|^2}{2l^2}\right)}_{\text{Base Kernel}} + \gamma \cdot \underbrace{\text{LLM}_{\text{coupling}}(\theta, \theta' | \mathcal{S})}_{\text{Coupling Term}}. \quad (5)$$

Analyze historical optimization data from P2D model simulations to adaptively guide parameter exploration. Identify highly sensitive parameters to voltage and dynamically adjust their search ranges, while maintaining wider exploration bounds for less sensitive parameters to avoid local optima. Enhance the expected improvement criterion by incorporating lithium-ion battery domain knowledge, such as penalizing unrealistic values. When generating candidate points, prioritize regions with high improvement potential while preserving global search capability. Ensure each iteration produces 15 candidate points to balance efficiency and thorough exploration.

Figure 4: Prompt for candidate sampling.

where  $l$  denotes the kernel length and  $\gamma$  represents the coupling strength. The coupling term  $\text{LLM}_{\text{coupling}}$  integrates electrochemical mechanisms as defined below:

$$\text{LLM}_{\text{coupling}} = \sum_{i,j} w_{ij} \cdot \frac{\partial U}{\partial \theta_i} \cdot \frac{\partial U}{\partial \theta_j} \quad (6)$$

where  $w_{ij}$  quantifies physical correlations. During optimization, the kernel length for sensitive parameters is reduced to capture abrupt voltage drops (as shown in Figure 3). The coupling strength at the  $(k+1)$ th iteration (denoted as  $\gamma_{k+1}$ ) adapts as follows:

$$\gamma_{k+1} = \gamma_k \cdot \left(1 + 0.1 \cdot \frac{f_{\min,k} - f_{\min,k-1}}{f_{\min,k-1}}\right) \quad (7)$$

where  $\gamma_k$  denotes the coupling strength at the  $k$ th iteration, and  $f_{\min,k}$  and  $f_{\min,k-1}$  are the best objective function value at the  $k$ th and  $(k-1)$ th iterations, respectively. As shown in Eq. (7), if  $f(\theta)$  converges rapidly,  $\gamma$  increases to strengthen coupling effects; otherwise,  $\gamma$  decreases to prevent overfitting.

### 3.4. LLM-enhanced candidate sampling

As depicted in Figure 4, to balance exploration and exploitation within the parameter space to effectively manage sensitive parameters, LLMBO dynamically adapts the acquisition function through contextual learning. Specifically, the expected improvement (EI) criterion is modified as follows:

$$\alpha_{\text{EI}}^{\text{LLM}}(\theta) = \mathbb{E} [\max(f_{\min} - f(\theta), 0)] \cdot \mathcal{W}_{\text{LLM}}(\theta | \mathcal{D}) \quad (8)$$

where  $f_{\min}$  denotes the objective function value of the best parameter in the current database (denoted as  $\mathcal{D}$ ), and  $\mathcal{W}_{\text{LLM}}$  is a weighting function generated by the LLM to prioritize sensitive parameters. Intuitively, if small variations in the parameters lead to significant fluctuations in the objective function value, the corresponding region is considered promising and should be assigned a higher weight. In view of this,  $\mathcal{W}_{\text{LLM}}$  is set as follows:

$$\mathcal{W}_{\text{LLM}} = \prod_{j=1}^q \frac{1}{\sqrt{2\pi\sigma_j^2}} \exp\left(-\frac{(\theta_j - \mu_j)^2}{2\sigma_j^2}\right) \quad (9)$$

where  $\mu_j$  and  $\sigma_j$  are the mean and standard deviation of the  $j$ th parameter, respectively. As shown in Eq. (9), a parameter vector containing parameters with smaller fluctuations is assigned a higher weight. Note that  $\mu_j$  and  $\sigma_j$  are dynamically adjusted to focus sampling on high-potential regions while preserving global exploration. Specifically,  $\mu_j$  is initialized based

---

### Algorithm 1: LLMBO

---

```

1  $t \leftarrow 0$ ;
2  $\mathcal{D} \leftarrow$  A database initialized by a random function and
   the LLM-based warm start;
3 Evaluate the parameters in  $\mathcal{D}$  using P2D simulations in
   accordance with Eq. (2);
4 while  $t \leq t_{\max} \&& f_{\min} \geq 10^{-3}$  do
5   Construct the composite kernel based on Eq. (5);
6   Construct the GP surrogate model;
7    $\mathcal{D}' \leftarrow$  LLM-enhanced candidate sampling;
8   Evaluate the parameters in  $\mathcal{D}'$  according to Eq. (2);
9   Update the database:  $\mathcal{D} \leftarrow \mathcal{D} \cup \mathcal{D}'$ ;
10   $t \leftarrow t + 1$ ;
11 end
12 Output the best parameter vector in  $\mathcal{D}$ ;

```

---

on prior knowledge and subsequently updated using newly sampled parameter vectors. To account for sensitive parameters, the value of  $\sigma_j$  is typically set to a small value initially, since high sensitivity often leads to large fluctuations. When the search tends to get trapped in a local optimum,  $\sigma_j$  is adaptively increased to encourage exploration.

### 3.5. Summary

The overall workflow of LLMBO for parameter identification is outlined in Algorithm 1.

First, a database (i.e.,  $\mathcal{D}$ ), consisting of 60 parameter vectors, is initialized using a random function and the LLM-based warm start. During the warm-start phase, the LLM's contextual learning ability is utilized to extract information from historical data and similar problems, providing more reasonable initial parameter values for the identification process rather than relying solely on random sampling. These parameters are evaluated using P2D simulations according to Eq. (2).

Next, the main loop begins with the construction of the composite kernel, as defined in Eq. (5), upon which the GP surrogate model is built. By adaptively tuning the kernel length for sensitive parameters, the influence of electrochemical mechanisms can be adjusted to enhance the accuracy of the GP surrogate model.

Subsequently, sample candidates according to the EI criterion enhanced by LLM. In this manner, LLMBO selects the most promising candidates from the parameter space based on the results of the previous identification round and suggestions from the LLM. These candidates are then simulated and evaluated using the P2D model.

Finally, the promising candidates are used to update the database. The main loop is repeated until a predefined stopping criterion is met. Specifically, the process terminates when the best objective function value satisfies  $f_{\min} < 10^{-3}$ , or when the number of iterations  $t$  exceeds the maximum limit  $t_{\max} = 50$ .

In summary, LLMBO continuously updates the database by optimizing parameters based on historical evaluation results and ultimately outputs the best parameter vector. Throughout

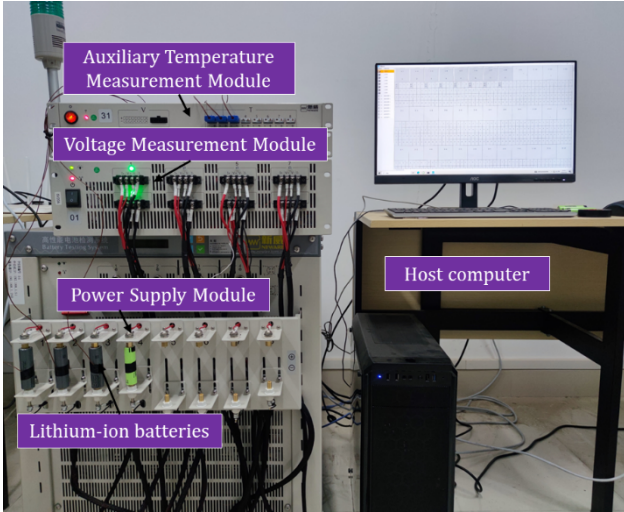


Figure 5: Experimental platform.

this process, it dynamically adapts both the surrogate model and candidate sampling strategy, thereby enhancing the efficiency of parameter identification and enabling relatively accurate results even in the early stages of identification.

## 4. Experimental study

### 4.1. Experiment setup

The effectiveness of LLMBO is demonstrated through a series of experiments conducted on an INR-21700-M50T battery, with specific parameters provided in Table 1. The NEWARE experimental platform, illustrated in Figure 5, was used to collect discharge voltage data under 0.5C, 1C, 2C, and 3C rates, which served as reference voltages for evaluation. The platform consists of five components: a power supply module, lithium-ion batteries, a voltage measurement module, an auxiliary temperature measurement module, and a host computer. The power supply module receives charging protocol information set by the host computer and delivers corresponding charge/discharge currents to the lithium-ion battery. The voltage measurement module and the auxiliary temperature measurement module collect data on the battery's voltage and temperature dynamics, respectively. In all discharge experiments, the initial state of charge (SOC) of the battery was set to 100%, and the discharge was terminated at a cutoff voltage of 2.5 V. All tests were conducted under room temperature conditions, with the ambient temperature maintained at approximately 298.15 K using an air-conditioned environment.

The P2D model was implemented using the Python Battery Mathematical Modeling (PyBaMM) software package. Additionally, LLMBO was implemented using Python version 3.10.20 on a laptop equipped with an Intel(R) Core(TM) i7-12700 CPU @ 2.30 GHz and 16 GB of RAM. The parameter settings of LLMBO are summarized in Table 2. In this study, six key dynamic parameters were identified. Specifically, active material volume fractions (i.e.,  $\varepsilon_{act,n}$  and  $\varepsilon_{act,p}$ ) directly impact electrode structural stability, diffusion coefficients (i.e.,  $D_{e,n}$  and

Table 1: INR-21700-M50T Battery Specifications

Parameter	Value
Nominal Capacity	5.0Ah
Upper cutoff voltage	4.2V
Lower cutoff voltage	2.5V
Length	70mm
Diameter	21mm
Internal Resistance	21.2mΩ

Table 2: Experimental parameter settings for LLMBO

Parameter	Value
Number of candidate solutions	15
Number of templates for generating solutions	2
Number of iterations for optimization	50
Parameter for controlling exploration-exploitation trade-off	-0.2
Number of initial samples	15
Number of trials	15
Engine used for chat-based tasks	GPT-3.5-Turbo/ DeepSeek-R1/GPT-4o
Percentage of top candidates to select	0.2

$D_{e,p}$ ) govern lithium-ion mobility, and solid phase conductivity parameters (i.e.,  $\sigma_{s,h}$  and  $\sigma_{s,p}$ ) determines electron transport efficiency. In summary, these parameters play a critical role in the management of lithium-ion batteries and have been widely investigated in the literature [38, 41]. Note that the sensitivity analysis in Section 4.2.4 highlights the importance of these six parameters. Since unreasonable parameter values may lead to simulation failures, it is essential to carefully set parameter ranges that have physical significance. The effective ranges are determined based on preliminary experiments and relevant literature [38, 41]. As a result, the effective ranges of these six parameters are summarized in Table 3. The following subsections present a detailed analysis of the experimental results.

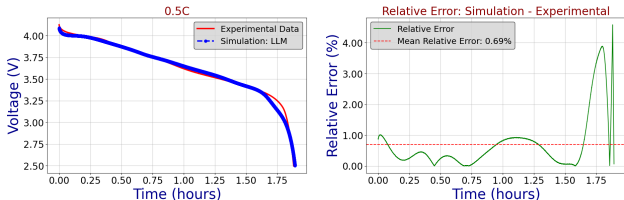
### 4.2. Results and discussions

#### 4.2.1. Identified results

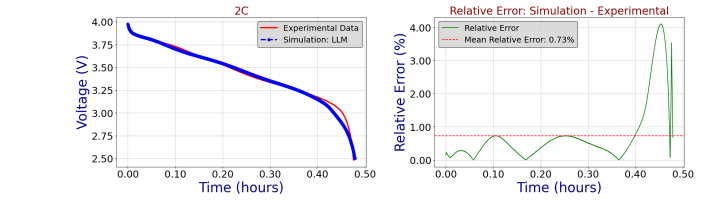
In this study, we implemented three versions of LLMBO, denoted as LLMBO-3.5, LLMBO-r1, and LLMBO-4o, utilizing GPT-3.5-Turbo, DeepSeek-R1, and GPT-4o (version 2024-08-06) as the respective inference engines. The identified results of LLMBO-3.5, LLMBO-r1, and LLMBO-4o are described in Table 3. We employed the parameters identified by LLMBO-4o to simulate the P2D model and compared the resulting voltages with reference voltages under various current rates, as illustrated in Figures 6 and 7. The results demonstrate a strong agreement between the simulated and reference voltages across different constant current rates, including 0.5C, 1C, 2C, and 3C. It is interesting to find that the relative error becomes noticeable at the end of discharge. Possible reasons for this phenomenon may include battery degradation and unknown disturbances. The battery used in the experiments may have experienced capacity degradation due to aging effects. Since the P2D model cannot capture degradation behavior without incorporating a thermal model [42], the loss of accuracy in capacity-related parameters may contribute to the observed prediction errors. Despite this impairment, the mean relative error remains

Table 3: The identified results of LLMBO and peer algorithms.

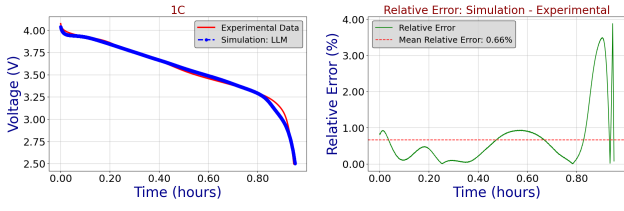
Parameters	Effective range	LLMBO-3.5	LLMBO-r1	LLMBO-4o	BO	PSO	GA
$\varepsilon_{act,p}$	[0.2,0.8]	6.64E-1	6.79E-1	6.87E-1	8.00E-1	7.20E-1	7.29E-1
$\varepsilon_{act,n}$	[0.2,0.8]	7.05E-1	7.14E-1	7.11E-1	8.00E-1	7.65E-1	7.16E-1
$D_{e,n}$	[1.0E-16,1.0E-12]	4.40E-14	5.71E-14	8.90E-14	1.00E-14	2.59E-14	4.72E-14
$D_{e,p}$	[1.0E-16,1.0E-12]	4.96E-14	2.63E-14	8.56E-15	1.00E-14	4.41E-15	5.79E-15
$\sigma_{s,n}$	[100,300]	2.38E+2	1.25E+2	2.22E+2	1.50E+2	2.34E+2	1.66E+2
$\sigma_{s,p}$	[0.2,0.8]	5.45E-1	4.68E-1	5.28E-1	3.00E-1	5.79E-1	3.29E-1



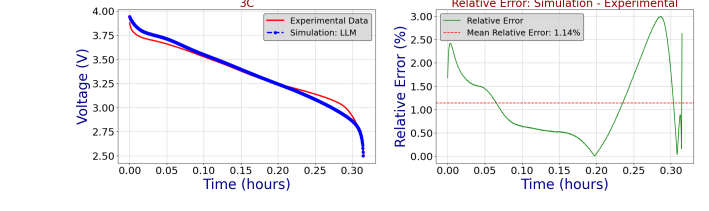
(a) Voltage comparison under 0.5C.



(a) Voltage comparison under 2C.



(c) Voltage comparison under 1C.



(b) Relative error under 2C.

(c) Voltage comparison under 3C.

(d) Relative error under 3C.

Figure 6: Simulation validation results under 0.5C and 1C.

Figure 7: Simulation validation results under 2C and 3C.

below 1.15%, indicating high accuracy in parameter identification.

#### 4.2.2. Performance comparison

To validate the effectiveness of LLMBO, we compared it with existing parameter identification algorithms, including BO [38], GA [22], and PSO [23]. We chose PSO and GA as baseline methods because they are well-established benchmark algorithms in battery parameter identification, with their performance extensively validated in the literature. All algorithms used identical values for shared hyperparameters, including the maximum number of iterations, stopping criterion, and other relevant configurations, to guarantee a fair comparison. Notably, during the 3C experiments, the peer algorithms, including BO, struggle to converge, requiring multiple trials to achieve satisfactory results. In contrast, LLMBO efficiently achieves better identification performance, benefiting from zero-shot warm start and the LLM’s dynamic adjustment of the acquisition function. Figure 8 evaluates the accuracy of the algorithms using error metrics, specifically root mean square error (RMSE) and mean absolute error (MAE), to facilitate a quantitative comparison. Figure 9 provides a comparative analysis of the computational time required by each algorithm during the identification process.

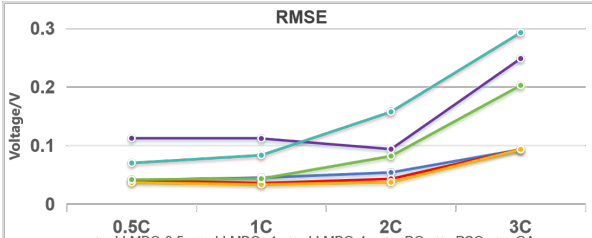
As shown in Figure 8, LLMBO-3.5, LLMBO-r1, and LLMBO-4o exhibit superior identification performance and significantly accelerate convergence. By effectively leverag-

ing historical information and prior knowledge, LLMBO is able to identify high-potential regions early in the process, thereby reducing the number of ineffective evaluations and enhancing overall identification efficiency.

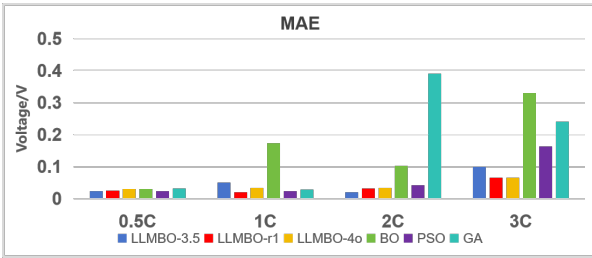
While traditional BO constructs a surrogate model using GP and employs a fixed acquisition function to achieve relatively good sample efficiency, its lack of dynamic adjustments and contextual adaptability makes it less effective in early-stage exploration. As a result, BO exhibits slower convergence and lower final accuracy compared to LLMBO.

Although PSO also delivers solid identification performance by relying on swarm intelligence for cooperative search, it tends to get trapped in local optima when dealing with nonlinear optimization problems. Additionally, PSO’s performance is highly sensitive to parameter settings, such as inertia weight and social parameters, which reduces its robustness and global search capability compared to LLMBO. Furthermore, GA’s dependency on manual parameter tuning for crossover probability and mutation intensity introduces additional optimization uncertainty, making it less adaptive compared to the gradient-aware mechanisms in LLMBO.

LLMBO-4o and LLMBO-r1, leveraging their multilevel contextual reasoning capabilities and dynamic semantic modeling mechanisms, demonstrate exceptional advantages in complex optimization tasks. They achieve the highest accuracy and fastest convergence speed while effectively reducing redundant exploration through physics-guided initialization strategies, re-



(a) RMSEs of LLMBO and peer algorithms



(b) MAEs of LLMBO and peer algorithms

Figure 8: Identification accuracy of LLMBO and peer algorithms.

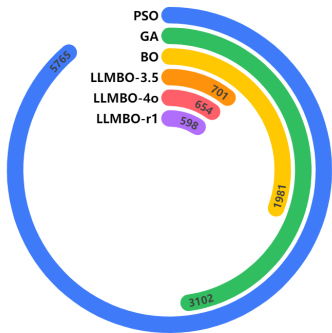


Figure 9: Computational time (s) of different algorithms for parameter identification.

sulting in more than a threefold improvement in overall efficiency compared to conventional methods. This positions GPT-4o and DeepSeek-R1 as optimal choices for parameter identification in advanced electrochemical systems. Despite offering the fastest single-inference speed, GPT-3.5-Turbo struggles to capture nonlinear electrochemical interactions due to its limited model capacity and context window, often resulting in convergence to local optima. The findings highlight that the depth of contextual understanding, dynamic adaptability, and task-specific compatibility of LLMs are critical determinants of their performance.

#### 4.2.3. Ablation study

Our prompt design consists of three fundamental components: (1) a description of the optimization problem, (2) the optimization history, and (3) explicit task instructions. To evaluate the impact of each component on performance, we conducted an ablation study with the following configurations:

Analyze historical optimization data from P2D model simulations to adaptively guide parameter exploration. Identify highly sensitive parameters to [voltage](#) and dynamically adjust their search ranges, while maintaining wider exploration bounds for less-sensitive parameters to avoid local optima. Enhance the expected improvement criterion by incorporating [lithium-ion battery domain knowledge](#), such as penalizing unrealistic values. When generating candidate points, prioritize regions with high improvement potential while preserving global search capability. Ensure each iteration produces 15 candidate points to balance efficiency and thorough exploration.

Figure 10: LLMBO[No context]: Prompt for the discriminative surrogate model with parts of the optimization problem description removed. Note that in this setting, no metadata about the underlying datasets is provided. Strikethrough indicates the component that is removed.

**Design a Bayesian optimization surrogate model that explicitly captures [electrochemical interactions in the P2D model](#).** Construct a composite kernel function combining a radial basis function with a coupling term based on porous electrode theory. For instance, model the synergistic effects between solid-phase diffusion and electrolyte volume fraction using gradient correlation analysis. Dynamically adjust hyperparameters: shorten the kernel length scale for parameters [causing voltage transients](#), and adapt the coupling strength based on convergence trends. Validate predictions against [multi-rate experimental voltage curves](#) to ensure physical consistency.

Figure 11: LLAMBO[No instructions]: Prompt for the candidate sampling with additional instructions removed. Strikethrough indicates the component that is removed.

- **LLMBO [No context]:** This variant assesses the impact of the optimization problem description on performance. Specifically, it omits metadata about the underlying dataset from the prompt (see Figure 10).
- **LLMBO [No instructions]:** In this setup, we excluded additional non-format-related instructions from the prompt. This includes removing guidelines in the candidate sampling regarding the type of points to sample. As a result, the retained instructions are purely to ensure compliance with the required format for regular processing (see Figure 11).

The experimental results in Figure 12 demonstrate that the standard LLMBO configuration outperforms the other variants, highlighting the importance of each prompt component in enhancing overall performance. Additionally, we observed that our ablation settings achieve competitive optimization performance compared to the baseline, with LLMBO [No context] being particularly notable. It exhibits similar optimization behavior even without any metadata about the underlying task. On one hand, this underscores the critical role of metadata about the dataset in guiding the optimization process. On the other hand, the robust performance of LLMBO [No context] despite the lack of metadata indicates the model’s effectiveness beyond relying on data memorization or leakage, as it operates without access to specific dataset information.

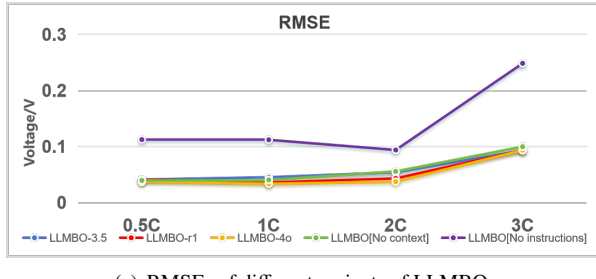
Furthermore, the inferior performance of LLMBO [No instructions] emphasizes the importance of detailed task instructions in improving the quality and efficiency of the candidate sampling process, ultimately contributing to overall optimization effectiveness.

#### 4.2.4. Further Discussions

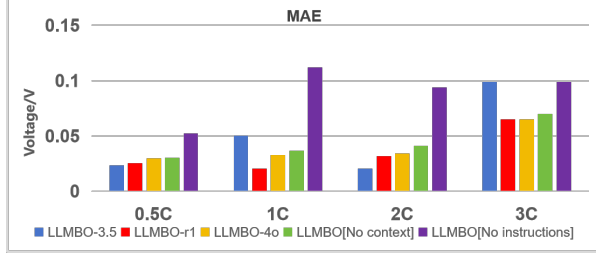
- To further analyze the impact of prompt design in the warm-start stage, we implemented a new variant, termed LLMBO-enhance1. In this variant, critical information,

Table 4: Identification accuracy of LLMBO-3.5, AO, BO, PSO, and GA, where the number of optimization iterations is set to {25, 50, 75}

Optimization iterations	LLMBO-3.5										AO										BO									
	0.5C		1C		2C		3C		0.5C		1C		2C		3C		0.5C		1C		2C		3C							
	RMSE	MAE	RMSE	MAE	RMSE	MAE	RMSE	MAE	RMSE	MAE	RMSE	MAE	RMSE	MAE	RMSE	MAE	RMSE	MAE	RMSE	MAE	RMSE	MAE	RMSE	MAE						
25	0.0312	0.0354	0.056	0.070	0.074	0.078	0.112	0.087	0.0477	0.0393	0.0784	0.0694	0.1227	0.0749	0.3461	0.2941	0.0432	0.0354	0.108	0.091	0.131	0.112	0.149	0.123						
50	0.0249	0.0297	0.049	0.059	0.063	0.064	0.094	0.075	0.0397	0.0328	0.0653	0.0578	0.1022	0.0625	0.2884	0.2451	0.0309	0.0351	0.064	0.069	0.107	0.099	0.135	0.110						
75	0.0205	0.0246	0.043	0.055	0.055	0.059	0.089	0.071	0.0358	0.0295	0.0588	0.0520	0.0920	0.0563	0.2595	0.2205	0.0248	0.0307	0.087	0.072	0.110	0.091	0.128	0.104						
PSO																														
Optimization iterations	GA																													
	0.5C		1C		2C		3C		0.5C		1C		2C		3C		0.5C		1C		2C		3C							
	RMSE	MAE	RMSE	MAE	RMSE	MAE	RMSE	MAE	RMSE	MAE	RMSE	MAE	RMSE	MAE	RMSE	MAE	RMSE	MAE	RMSE	MAE	RMSE	MAE	RMSE	MAE						
25	0.0607	0.0679	0.113	0.096	0.138	0.117	0.155	0.129	0.0678	0.0761	0.121	0.103	0.145	0.124	0.162	0.133	0.0642	0.0671	0.108	0.091	0.131	0.112	0.149	0.123						
50	0.0442	0.0516	0.098	0.083	0.122	0.104	0.140	0.116	0.0516	0.0589	0.106	0.091	0.130	0.112	0.147	0.123	0.0309	0.0351	0.064	0.069	0.107	0.099	0.135	0.110						
75	0.0335	0.0401	0.091	0.076	0.115	0.096	0.133	0.109	0.0387	0.0452	0.099	0.084	0.123	0.103	0.139	0.117	0.0248	0.0307	0.087	0.072	0.110	0.091	0.128	0.104						



(a) RMSEs of different variants of LLMBO



(b) MAEs of different variants of LLMBO

Figure 12: Identification accuracy of LLMBO and the variants.

As an electrochemistry expert, generate an initial parameter set for the pseudo-two-dimensional model of an INR-21700-M50T lithium-ion battery (NMC811 cathode/graphite anode). Integrate the following constraints: positive electrode thickness = 73μm, negative electrode thickness = 85μm, separator thickness = 12μm; ensure active material volume fractions ( $\varepsilon_{act,p}, \varepsilon_{act,n}$ ) satisfy 0.2–0.8 range with  $\varepsilon_{act,p} + \varepsilon_{act,n} \leq 1$ , electrolyte diffusion coefficients ( $D_{e,p}, D_{e,p}$ ) maintained within  $10^{-16}$ – $10^{-12}$  m<sup>2</sup>/s range, and solid-phase conductivity aligned with electrode material properties. Generate physically feasible and diverse parameter combinations based on prior literature knowledge while strictly avoiding invalid configurations.

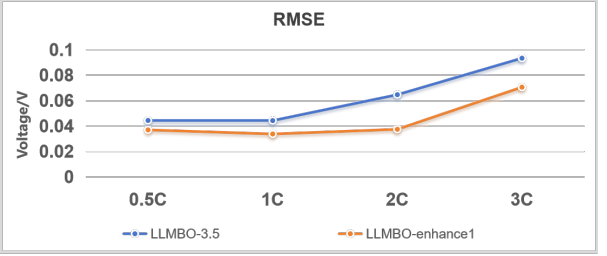
Figure 13: LLMBO-enhance1: Prompt with additional critical information for warm start.

such as cell chemistry and form factors, was incorporated into the prompt as key inputs, as illustrated in Figure 13. The results in Figure 14 demonstrate that LLMBO-enhance1 consistently outperforms the original LLMBO-3.5 across all C-rates in terms of both RMSE and MAE. Additionally, LLMBO-enhance1 is more efficient than LLMBO-3.5. For instance, under the 1C rate condition, it completes in 598.6 seconds, compared to 701 seconds required by LLMBO-3.5. The results demonstrate that incorporating additional critical information into the prompt can further improve both the accuracy and efficiency of LLMBO.

- To validate the effectiveness of the composite kernel, we compared the performance of the traditional BO with BO incorporating the composite kernel (denoted as BO-

Table 5: Running time of LLMBO-3.5, AO, BO, PSO, and GA, where the number of optimization iterations is set to {25, 50, 75}

Optimization Iterations	LLMBO-3.5	AO	BO	PSO	GA
25	435 s	480 s	792 s	2958 s	1764 s
50	701 s	960 s	1981 s	5765 s	3102 s
75	1099 s	1440 s	2461 s	10325 s	4931 s



(a) RMSEs of LLMBO-enhance1 and LLMBO-3.5

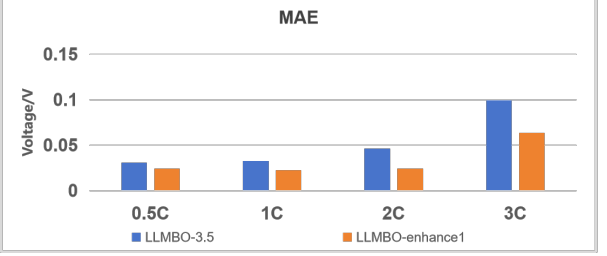
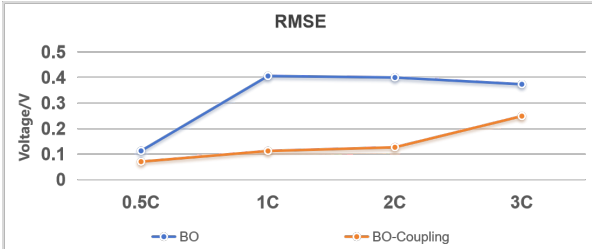


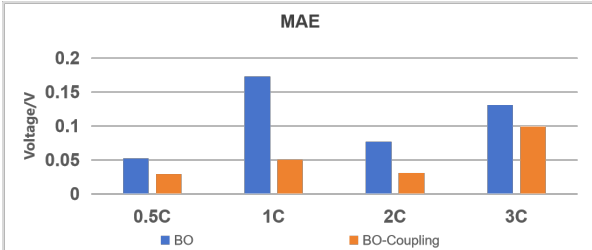
Figure 14: Identification accuracy of LLMBO-enhance1 and LLMBO-3.5.

Coupling). It can be seen from Figure 15 that BO-Coupling achieves lower prediction errors, with the final RMSE and MAE values markedly reduced compared to the traditional BO. This advantage stems from the inherent strong nonlinear coupling characteristics of electrochemical model parameters. Conventional kernels rely solely on Euclidean distance to measure similarity, which fail to capture physical interaction relationships. In contrast, the gradient coupling term introduced in the composite kernel dynamically adjusts the definition of parameter similarity, with weights determined by the sensitivity of parameters to model responses. This mechanism enhances the optimization efficiency of the surrogate model. In summary, the results demonstrate that the composite kernel significantly enhances optimization performance through gradient coupling mechanisms.

- To further validate the efficacy of LLMBO, we introduced a state-of-the-art metaheuristic, i.e., the artificial



(a) RMSEs of BO and BO-Coupling.

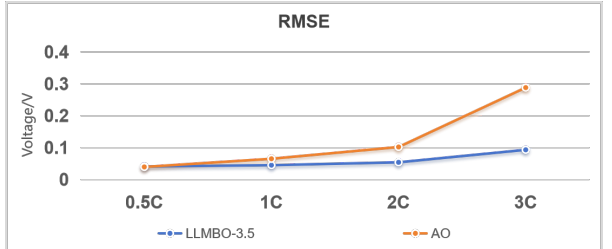


(b) MAEs of BO and BO-Coupling.

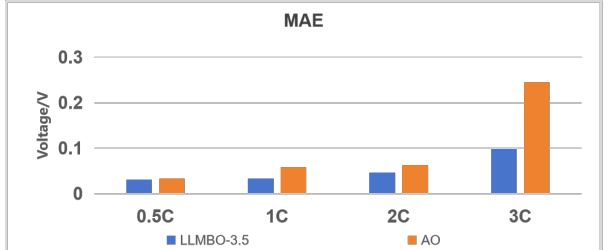
Figure 15: Identification accuracy of BO and BO-Coupling.

Owl (AO) algorithm [43], as an additional competitor. Given its demonstrated effectiveness across a range of engineering optimization tasks, AO serves as a representative advanced optimizer for a systematic comparison with LLMBO. Experimental results in Figure 16 indicate that AO performs inferiorly to LLMBO in both accuracy and stability. In contrast, LLMBO consistently achieves lower RMSE and MAE values, highlighting its superior generalization capability in battery parameter identification tasks.

- To mitigate potential biases arising from a single hyperparameter configuration, we expanded the experimental design by evaluating three additional settings beyond the default case. Specifically, the number of optimization iterations was set to 25, 50, and 75 to assess performance under varying computational budgets. To ensure a fair comparison, all methods were implemented using identical values for shared hyperparameters. As shown in Table 4, LLMBO consistently achieves better results across all iteration settings. Moreover, the time costs reported in Table 5 indicate that LLMBO requires less computational effort compared to peer algorithms.
- To quantify the influence of key parameters in the lithium-ion battery model for the given cell, we conducted a global sensitivity analysis using the Morris method [44]. This approach quantifies parameter influence using the  $\mu^*$  metric, which represents the *average magnitude of elementary effects* on output responses—higher  $\mu^*$  values indicate greater parameter sensitivity. As visualized in Figure 17, for the given cell, the six selected parameters exhibit higher  $\mu^*$  values than the alternatives. These mechanistically grounded targets provide critical prioritization for efficient battery model



(a) RMSEs of LLMBO-3.5 and AO



(b) MAEs of LLMBO-3.5 and AO

Figure 16: Identification accuracy of LLMBO-3.5 and AO.

identification.

- To validate the impact of battery variations, specifically differences in aging stage, on parameter identification, we conducted experiments on three INR-21700-M50T batteries at different aging stages (i.e., after 0, 140, and 260 charge-discharge cycles). The proposed LLMBO was compared with peer algorithms. Experimental results demonstrate that LLMBO consistently achieves superior parameter identification accuracy across all aging levels (see Figure 18). These findings highlight LLMBO’s strong adaptability to battery state variations, making it a reliable modeling solution under complex operational conditions.

## 5. Conclusions

In this paper, we make the first attempt to combine LLMs with BO for parameter identification of the P2D model. Specifically, we design tailored prompts to enhance each component of BO and propose three strategies: LLM-based warm start, LLM-enhanced surrogate modeling, and LLM-enhanced candidate sampling. By leveraging the synergistic optimization capabilities of LLMs and BO, the proposed LLMBO achieves faster convergence, higher accuracy, and superior sample efficiency in lithium-ion battery parameter identification. Experimental results demonstrate that LLMBO is more efficient than traditional BO and more stable than other heuristic algorithms, thereby providing a new research direction for parameter identification in complex physical systems. Furthermore, we systematically analyze the performance differences among multiple LLMs in the parameter identification task. The results reveal that GPT-4o and DeepSeek-R1, owing to their advanced contextual reasoning capabilities, outperform other models. Notably, with

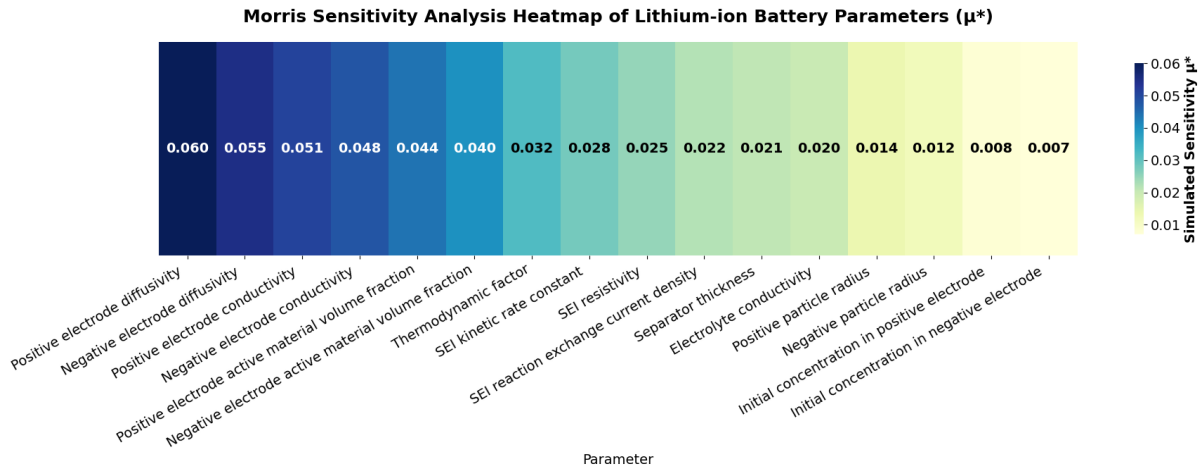


Figure 17: Morris Sensitivity indices for key parameters

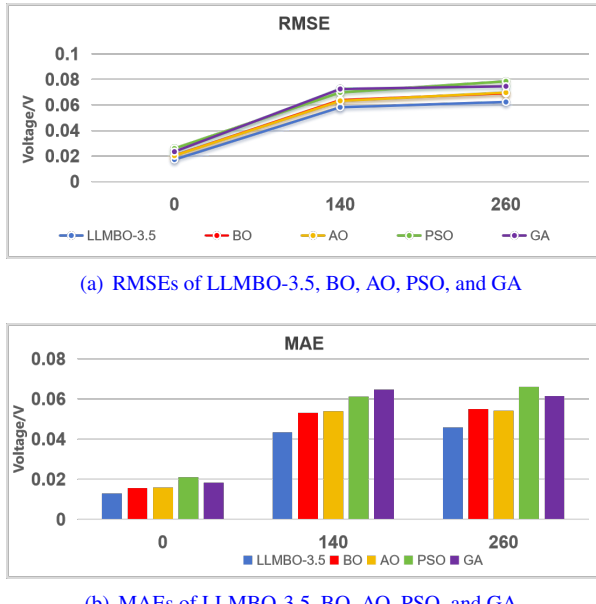


Figure 18: Identification accuracy of LLMBO-3.5, BO, AO, PSO, and GA for batteries at different aging stages.

the rapid advancement of LLMs, their optimization capabilities have also significantly improved. In the future, this approach can be extended to higher-dimensional optimization tasks with even more complex search spaces.

#### COMPLETE PROMPTS

Here's the translation of key prompts for each BO component, maintaining technical accuracy while ensuring clarity for electrochemical applications:

1. Integrate electrochemical constraints and material properties to generate physically feasible initial parameter sets (Figure 2).
2. Construct composite kernel functions incorporating porous electrode theory, correlating parameter coupling

through voltage gradients, and coupling strength to capture voltage transient features (Figure 3).

3. Dynamically adjust parameter search ranges by prioritizing exploration of high-potential regions based on sensitivity analysis while maintaining global random sampling to balance exploration and exploitation (Figure 4).

It should be noted that the prompts presented in the article represent only the key components and do not include input/output formats or implementation details. The system innovatively encodes electrochemical mechanisms into the prompt design, with physical consistency validated through multi-rate voltage curves, thereby pioneering new approaches for lithium-ion battery parameter identification.

#### Nomenclature

$\theta$	parameter vector consisting of battery model parameters
$\theta_k$	$k$ th candidate parameter vector
$f(\theta), f(\theta_k)$	objective function values of $\theta$ and $\theta_k$ , respectively
$\underline{\theta}_j, \bar{\theta}_j$	lower and upper bounds of the $j$ th parameter $\theta_j$ , respectively
$U^{\text{ref}}$	vector of experimentally observed voltages
$U$	vector of reference voltages generated by the P2D model
$U_i, U_i^{\text{ref}}$	$i$ th samples of the measured voltages and the reference voltages, respectively

$q$	number of parameters
$n$	number of samples
$\varepsilon_{act,p}$	positive electrode active material volume fraction
$\varepsilon_{act,n}$	negative electrode active material volume fraction
$\varepsilon_{e,p}$	volume fraction of the electrolyte phase in the positive electrode
$\mathcal{P}_{LLM}$	LLM-based parser responsible for analyzing a constraint set
$\mathcal{S}$	domain-specific semantic constraints
$k(\theta, \theta')$	composite kernel function of $\theta$ and $\theta'$
$LLM_{coupling}$	coupling term in the composite kernel function
$l$	kernel length in the composite kernel function
$\gamma$	coupling strength in the composite kernel function
$w_{ij}$	quantification of physical correlations in the coupling term
$f_{\min,k}$	best objective function value at the $k$ th iteration
$\mathcal{D}$	database of parameter vectors
$f_{\min}$	best objective function value in the database $\mathcal{D}$
$\alpha_{EI}^{LLM}(\theta)$	LLM-enhanced expected improvement value of $\theta$
$\mathcal{W}_{LLM}$	weighting function generated by the LLM to prioritize sensitive parameters
$\mathcal{D}'$	database of new sampling parameter vectors
$t_{\max}$	maximum iteration number
$D_{e,n}$	negative electrode diffusivity
$D_{e,p}$	positive electrode diffusivity
$\sigma_{s,n}$	negative electrode conductivity
$\sigma_{s,p}$	positive electrode conductivity

- a gbls booster multi-task model, Journal of Energy Storage 75 (2024) 109741.
- [2] D. Larcher, J.-M. Tarascon, Towards greener and more sustainable batteries for electrical energy storage, Nature Chemistry 7 (1) (2015) 19–29.
  - [3] S. Zhang, X. Zhang, A comparative study of different online model parameters identification methods for lithium-ion battery, Science China Technological Sciences 64 (10) (2021) 2312–2327.
  - [4] L. Chen, W. Shen, Y. Zhou, X. Mou, L. Lei, Learning-based sparse spatiotemporal modeling for distributed thermal processes of lithium-ion batteries, Journal of Energy Storage 69 (2023) 107834.
  - [5] J. Newman, K. E. Thomas, H. Hafezi, D. R. Wheeler, Modeling of lithium-ion batteries, Journal of Power Sources 119 (2003) 838–843.
  - [6] L. A. Román-Ramírez, J. Marco, Design of experiments applied to lithium-ion batteries: A literature review, Applied Energy 320 (2022) 119305.
  - [7] M. J. Lain, E. Kendrick, Understanding the limitations of lithium ion batteries at high rates, Journal of Power Sources 493 (2021).
  - [8] A. I. Rodriguez-Cea, D. Morinigo-Sotelo, F. V. Tinaut, A procedure for evaluating the soh of li-ion batteries from data during the constant voltage charge phase and the use of an ecm with internal resistance, Journal of Energy Storage 108 (2025) 115074.
  - [9] J. Newman, W. Tiedemann, Porous-electrode theory with battery applications, AIChE Journal 21 (1) (1975) 25–41.
  - [10] J. Newman, N. P. Balsara, Electrochemical Systems, John Wiley & Sons, 2021.
  - [11] R. Krishna, J. A. Wesselingh, The maxwell-stefan approach to mass transfer, Chemical Engineering Science 52 (6) (1997) 861–911.
  - [12] D. Zhang, B. N. Popov, R. E. White, Modeling lithium intercalation of a single spinel particle under potentiodynamic control, Journal of the Electrochemical Society 147 (3) (2000) 831.
  - [13] M. Guo, G. Sikha, R. E. White, Single-particle model for a lithium-ion cell: Thermal behavior, Journal of The Electrochemical Society 158 (2) (2010) A122.
  - [14] S. K. Rahimian, S. Rayman, R. E. White, Extension of physics-based single particle model for higher charge–discharge rates, Journal of Power Sources 224 (2013) 180–194.
  - [15] G.-H. Kim, K. Smith, K.-J. Lee, S. Santhanagopalan, A. Pesaran, Multi-domain modeling of lithium-ion batteries encompassing multi-physics in varied length scales, Journal of the Electrochemical Society 158 (8) (2011) A955.
  - [16] M. Torchio, L. Magni, R. B. Gopaluni, R. D. Braatz, D. M. Raimondo, Lionsimba: a matlab framework based on a finite volume model suitable for li-ion battery design, simulation, and control, Journal of The Electrochemical Society 163 (7) (2016) A1192.
  - [17] L. Cai, R. E. White, Reduction of model order based on proper orthogonal decomposition for lithium-ion battery simulations, Journal of the Electrochemical Society 156 (3) (2008) A154.
  - [18] P. W. Northrop, V. Ramadesigan, S. De, V. R. Subramanian, Coordinate transformation, orthogonal collocation, model reformulation and simulation of electrochemical-thermal behavior of lithium-ion battery stacks, Journal of The Electrochemical Society 158 (12) (2011) A1461.
  - [19] A. M. Bizeray, S. Zhao, S. R. Duncan, D. A. Howey, Lithium-ion battery thermal-electrochemical model-based state estimation using orthogonal collocation and a modified extended kalman filter, Journal of Power Sources 296 (2015) 400–412.
  - [20] G.-H. Kim, K. Smith, J. Lawrence-Simon, C. Yang, Efficient and extensible quasi-explicit modular nonlinear multiscale battery model: Gh-msmd, Journal of The Electrochemical Society 164 (6) (2017) A1076.
  - [21] J. Li, Y. Peng, Q. Wang, H. Liu, Status and prospects of research on lithium-ion battery parameter identification, Batteries 10 (6) (2024) 194.
  - [22] J. Li, L. Zou, F. Tian, X. Dong, Z. Zou, H. Yang, Parameter identification of lithium-ion batteries model to predict discharge behaviors using heuristic algorithm, Journal of The Electrochemical Society 163 (8) (2016) A1646.
  - [23] M. A. Rahman, S. Anwar, A. Izadian, Electrochemical model based fault diagnosis of lithium ion battery, Dissertations & Theses Gradworks (2016).
  - [24] H. Chun, J. Kim, S. Han, Parameter identification of an electrochemical lithium-ion battery model with convolutional neural network, IFAC-PapersOnLine 52 (4) (2019) 129–134.
  - [25] Y. Wang, Q. Yao, J. T. Kwok, L. M. Ni, Generalizing from a few ex-

## References

- [1] P. Yang, H. Yang, X. Meng, C. Song, T. He, J. Cai, Y. Xie, K. Xu, Joint evaluation and prediction of soh and rul for lithium batteries based on

- amples: A survey on few-shot learning, *ACM computing surveys (csur)* 53 (3) (2020) 1–34.
- [26] T. Brown, B. Mann, N. Ryder, M. Subbiah, J. D. Kaplan, P. Dhariwal, A. Neelakantan, P. Shyam, G. Sastry, A. Askell, et al., Language models are few-shot learners, *Advances in Neural Information Processing Systems* 33 (2020) 1877–1901.
- [27] S. Holt, M. R. Luyten, M. van der Schaar, L2mac: Large language model automatic computer for extensive code generation, *arXiv preprint arXiv:2310.02003* (2023).
- [28] N. Seedat, N. Huynh, B. Van Breugel, M. Van Der Schaar, Curated llm: Synergy of llms and data curation for tabular augmentation in low-data regimes, *arXiv preprint arXiv:2312.12112* (2023).
- [29] G. Penedo, Q. Malartic, D. Hesslow, R. Cojocaru, A. Cappelli, H. Alobaidi, B. Pannier, E. Almazrouei, J. Launay, The refinedweb dataset for falcon llm: outperforming curated corpora with web data, and web data only, *arXiv preprint arXiv:2306.01116* (2023).
- [30] A. Chowdhery, S. Narang, J. Devlin, M. Bosma, G. Mishra, A. Roberts, P. Barham, H. W. Chung, C. Sutton, S. Gehrmann, et al., Palm: Scaling language modeling with pathways, *Journal of Machine Learning Research* 24 (240) (2023) 1–113.
- [31] J. Wei, X. Wang, D. Schuurmans, M. Bosma, F. Xia, E. Chi, Q. V. Le, D. Zhou, et al., Chain-of-thought prompting elicits reasoning in large language models, *Advances in Neural Information Processing Systems* 35 (2022) 24824–24837.
- [32] J. Wei, Y. Tay, R. Bommasani, C. Raffel, B. Zoph, S. Borgeaud, D. Yogatama, M. Bosma, D. Zhou, D. Metzler, et al., Emergent abilities of large language models, *arXiv preprint arXiv:2206.07682* (2022).
- [33] V. Sanh, A. Webson, C. Raffel, S. H. Bach, L. Sutawika, Z. Alyafeai, A. Chaffin, A. Stiegler, T. L. Scao, A. Raja, et al., Multitask prompted training enables zero-shot task generalization, *arXiv preprint arXiv:2110.08207* (2021).
- [34] L. Ouyang, J. Wu, X. Jiang, D. Almeida, C. Wainwright, P. Mishkin, C. Zhang, S. Agarwal, K. Slama, A. Ray, et al., Training language models to follow instructions with human feedback, *Advances in Neural Information Processing Systems* 35 (2022) 27730–27744.
- [35] T. Liu, N. Astorga, N. Seedat, M. van der Schaar, Large language models to enhance bayesian optimization, *arXiv preprint arXiv:2402.03921* (2024).
- [36] M. Doyle, T. F. Fuller, J. Newman, Modeling of galvanostatic charge and discharge of the lithium/polymer/insertion cell, *Journal of the Electrochemical society* 140 (6) (1993) 1526.
- [37] A. Jokar, B. Rajabloo, M. Désilets, M. Lacroix, Review of simplified pseudo-two-dimensional models of lithium-ion batteries, *Journal of Power Sources* 327 (2016) 44–55.
- [38] Zhou, Yu et. al, A Surrogate-Assisted Teaching-Learning-Based Optimization for Parameter Identification of the Battery Model, *IEEE Transactions on Industrial Informatics* 17 (9) (2021) 5909–5918. doi:10.1109/TII.2020.3038949.
- [39] B. Shahriari, K. Swersky, Z. Wang, R. P. Adams, N. De Freitas, Taking the human out of the loop: A review of bayesian optimization, *Proceedings of the IEEE* 104 (1) (2015) 148–175.
- [40] B.-C. Wang, Y.-B. He, J. Liu, B. Luo, Fast parameter identification of lithium-ion batteries via classification model-assisted bayesian optimization, *Energy* 288 (2024) 129667.
- [41] C.-H. Chen, F. B. Planella, K. O’regan, D. Gastol, W. D. Widanage, E. Kendrick, Development of experimental techniques for parameterization of multi-scale lithium-ion battery models, *Journal of The Electrochemical Society* 167 (8) (2020) 080534.
- [42] T. M. Bandhauer, S. Garimella, T. F. Fuller, A critical review of thermal issues in lithium-ion batteries, *Journal of the Electrochemical Society* 158 (3) (2011) R1.
- [43] Abualigah, Laith et. al, Aquila optimizer: a novel meta-heuristic optimization algorithm, *Computers & Industrial Engineering* 157 (2021) 107250.
- [44] King, David Michael and Perera, BJC, Morris method of sensitivity analysis applied to assess the importance of input variables on urban water supply yield—A case study, *Journal of hydrology* 477 (2013) 17–32.